Macromolecules **1985**, *18*, 2068–2072

Characterization of Styrene–Divinylbenzene Copolymers by High-Resolution Pyrolysis–Gas Chromatography

Hiroshi Nakagawa and Shin Tsuge*

Department of Synthetic Chemistry, Faculty of Engineering, Nagoya University, Nagoya 464, Japan. *Received September 28, 1984*

ABSTRACT: Pyrolysis–gas chromatography (PyGC) with a high-resolution fused-silica capillary column was utilized to investigate styrene–divinylbenzene (ST–DVB) copolymers. The assigned characteristic peaks up to styrene trimer were interpreted not only with respect to the compositional determination but also with respect to the network structures. Thermogravimetric analysis (TGA) and differential scanning calorimetry (DSC) were also utilized to measure the thermal behavior of the ST–DVB copolymers.

Styrene–divinylbenzene (ST–DVB) copolymers with tridimensional structures are extensively used in the area of ion-exchange chromatography, gel permeation chromatography, and gas chromatography. Because of their intractable network structures, however, characterization has been extremely restricted. Rietsch et al.[1–7] studied the physicochemical properties of anionically prepared ST–DVB copolymers with varying number-average molecular weights ($\bar{M}_n$) between the networks and various functionalities of the cross-links. These studies included measurements of the glass transition temperature (T_g), swelling ratio, and elastic behavior in the swollen or dry state. The experimental results were interpreted in terms of established physicochemical theories. The influence of free chains in the networks on the physicochemical properties was also discussed.

On the other hand, Sellier et al.[8] studied ST–DVB copolymers by pyrolysis–gas chromatography (PyGC) with a capillary column. Among the various characteristic products on the pyrograms, they used the ratio of monomeric styrene to toluene as a measure of the DVB content in the copolymers. Häusler et al.[9] also characterized ST–DVB copolymers cross-linked by methylene groups by means of conventional PyGC, where styrene and *m*- and *p*-ethyltoluene plus *p*-cymene were used as characteristic products of non-cross-linked and cross-linked fractions, respectively. They suggested that ST–DVB copolymers prepared by suspension and solution copolymerization could be differentiated. The pyrograms in both PyGC studies mentioned above, however, only covered the associated monomeric products from the copolymers, and their peak resolution was not high enough to develop detailed discussion on the network structures.

In this paper, ST–DVB copolymers with varying DVB content prepared by radical copolymerization were studied by PyGC with a high-resolution fused-silica capillary column. The obtained high-resolution pyrograms that cover up to the region of styrene trimer were interpreted not only with respect to the compositional determination but also with respect to the network structures. In addition, thermogravimetric analysis (TGA) and differential scanning calorimetry (DSC) were carried out to measure the thermal behavior of the ST–DVB copolymers.

Experimental Section

Conditions for PyGC. A vertical microfurnace-type pyrolyzer (Yanagimoto GP-1018) directly attached to a gas chromatograph (Yanagimoto G-3800) with flame ionization detectors was used in this study. Details of the PyGC system were essentially the same as described elsewhere.[10] A high-resolution fused-silica capillary column (0.25 mm i.d. × 25 m long) wall coated with OV-101 was used in a temperature programming mode from 50 to 250 °C at a rate of 3 °C/min. The flow rate (30 mL/min) of the nitrogen carrier gas at the pyrolyzer was reduced to 1.2 mL/min at the capillary column through a splitter. The glass insert in the injection port of the gas chromatograph was packed with supporting material, Diasolid-H (80/100 mesh) coated with 5% OV-101 and held at 250 °C in order to protect the capillary column from contamination by the high boiling point tarry pyrolyzates. Samples of about 150 μg were pyrolyzed at 590 °C. The peak areas of the resultant pyrograms were integrated by an integrator (Shimadzu Chromatopac E-1A), and the peak identification was primarily carried out by a GC–MS system (JEOL JMS-DX300) attached to the pyrolyzer.

Table I
ST-DVB Copolymer Samples

	composition, wt %		
sample	ST	DVB's	EST's
A	98.2	1.0	0.8
B	96.4	2.0	1.6
C	81.8	10.0	8.2
D	67.3	18.0	14.7
E	54.5	25.0	20.5
F	40.0	33.0	27.0
G		55.0	45.0
H	89.0	11.0	

Conditions for TGA and DSC. TGA measurements were carried out with a Rigaku-Denki thermobalance. About 8 mg of the sample weighed in a platinum dish was measured from room temperature to about 600 °C at a rate of 10 °C/min under a gentle flow of nitrogen. T_g measurements were made on a Rigaku-Denki differential scanning calorimeter (DSC-8230). About 10 mg of the sample was measured from room temperature to about 200 °C at a rate of 5 °C/min under a flow of nitrogen (30 mL/min).

Materials. The eight kinds of ST–DVB copolymer samples utilized are listed in Table I together with their compositions. Samples A–F were synthesized by conventional radical copolymerization of styrene (ST) and divinylbenzenes (DVB's) that contained 45.0 wt % ethylstyrenes (EST's). Sample G was prepared only from the DVB's containing 45.0 wt % EST's. A reference copolymer sample H was synthesized from ST and DVB's free from EST's. Samples A–E and G were provided by Showa-Denko Industry Inc. and samples F and H by Toyo-Soda Industry Inc. In addition, monodisperse linear polystyrenes (PS's) ranging from $\bar{M}_n$ ($\approx\bar{M}_w$) = 900–860 000 supplied by Waters Co. Ltd. were also used as reference polymers for estimating the weight-average molecular weight ($\bar{M}_w$) of ST sequences in the networks of the ST–DVB copolymers.

Results and Discussion

General Thermal Degradation Behavior of ST–DVB Copolymers. Figure 1 shows typical high-resolution pyrograms of ST–DVB copolymers with different ST content (samples H, C, E, and G). The peak assignments of the pyrograms are summarized in Table II. The intensities of the ST monomer (peak 3), dimer (peak 13), and trimer (peak 16), which are characteristic of ST sequences, decrease with the rise of DVB content, while those of methylstyrenes (MST's) (peaks 6 and 7), EST's (peaks 8 and 9), and DVB's (peaks 10 and 11) show the opposite tendency. In addition, hybrid dimers between ST, DVB's, and EST's (cluster peak 14), dimers of DVB's or EST's and hybrid dimers between DVB's and EST's (cluster peak

0024-9297/85/2218-2068$01.50/0 © 1985 American Chemical Society

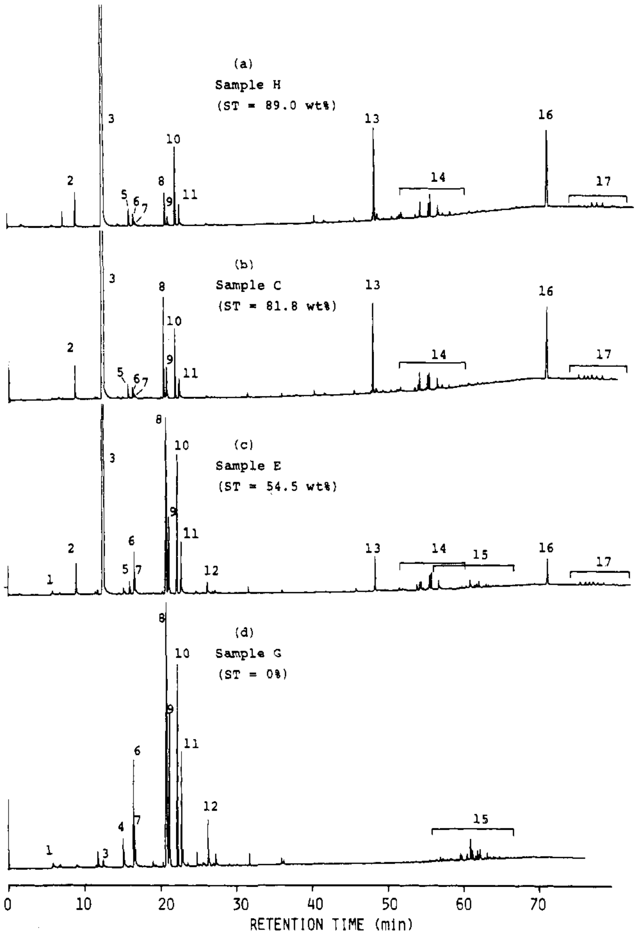

Figure 1. High-resolution pyrograms of ST–DVB copolymers. Peak numbers are consistent with those in Table II.

Table II
Peak Assignment on the Pyrograms of ST-DVB Copolymers

peak no.	peak assign	structure
1	hydrocarbons (C_1–C_4)	
2	toluene	C–Ph
3	styrene	C=C–Ph
4	isopropylbenzene	C–C(C)–Ph
5	*α*-methylstyrene	C=C(C)–Ph
6	*m*- and *p*-methylstyrene	C=C–C_6H_4–C
7	*o*-methylstyrene	C=C–C_6H_4–C
8	*m*- and *p*-ethylstyrene	C=C–C_6H_4–C–C
9	*o*-ethylstyrene	C=C–C_6H_4–C–C
10	*m*- and *p*-divinylbenzene	C=C–C_6H_4–C=C
11	*o*-divinylbenzene	C=C–C_6H_4–C=C
12	*m*- and *p*-isopropenylstyrene	C=C(C)–C_6H_4–C=C
13	2,4-diphenyl-1-butene (styrene dimer)	C=C(Ph)–C–C–Ph
14	hybrid dimers between ST, DVB's and EST's	
15	dimers of DVB's or EST's and hybrid dimers between DVB's and EST's	
16	2,4,6-triphenyl-1-hexene (styrene trimer)	C=C(Ph)–C–C(Ph)–C–C–Ph
17	hybrid trimers between ST, DVB's, and EST's	

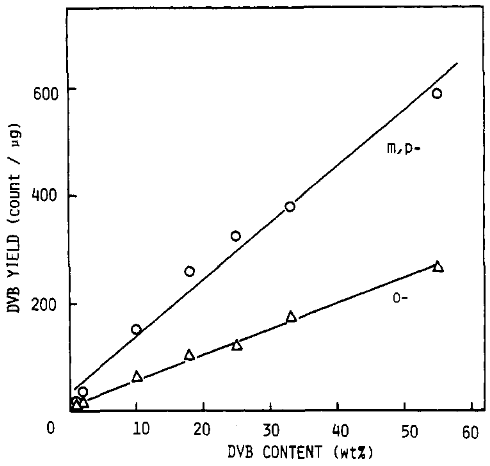

Figure 2. Relationship between DVB isomer yields and DVB content of ST–DVB copolymers.

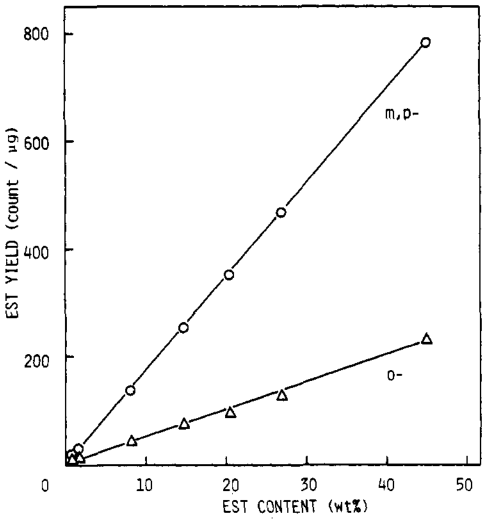

Figure 3. Relationship between EST isomer yields and EST content of ST–DVB copolymers.

15), and hybrid trimers between ST, DVB's, and EST's (cluster peak 17) are observed on the pyrograms depending on the composition of the copolymers.

It is interesting to note that fairly strong EST peaks (peaks 8 and 9) are observed even on the pyrogram of (a) for sample H, which does not contain any EST units. This phenomenon suggests that the DVB units in the network of the copolymers yield EST's in addition to DVB's through competitive thermal reactions. Similarly, MST's on the pyrograms (peaks 6 and 7) might also be formed from DVB units.

Determination of the Copolymer Composition. Figure 2 shows the relationships between the DVB content of the copolymers and observed yields of DVB isomers on the pyrograms. The DVB yields (Y_{DVB}) are defined as follows by normalizing the associated peak intensities (counts) (I_{DVB}) by the sample amount, w (μg):

$$Y_{m\text{-},p\text{-DVB}} = I_{m\text{-},p\text{-DVB}}/w$$
$$Y_{o\text{-DVB}} = I_{o\text{-DVB}}/w \qquad (1)$$

Similarly, the relationships between the EST content of the copolymers and the yield of the EST isomers are shown in Figure 3. In this case the yields of EST (Y_{EST}) were calculated from the observed peak intensity (I_{EST}) by correcting the contribution from DVB units discussed above for the pyrogram of sample H in Figure 1

$$Y_{m\text{-},p\text{-EST}} = (I_{m\text{-},p\text{-EST}} - 0.426 I_{m\text{-},p\text{-DVB}})/w$$
$$Y_{o\text{-EST}} = (I_{o\text{-EST}} - 0.419 I_{o\text{-DVB}})/w \qquad (2)$$

where 0.426 and 0.419 are the correction factors for the contribution of *m*-,*p*-DVB to *m*-,*p*-EST and *o*-DVB to *o*-EST, respectively. The correction factor 0.426, for example, for the contribution of *m*-,*p*-DVB to *m*-,*p*-EST is

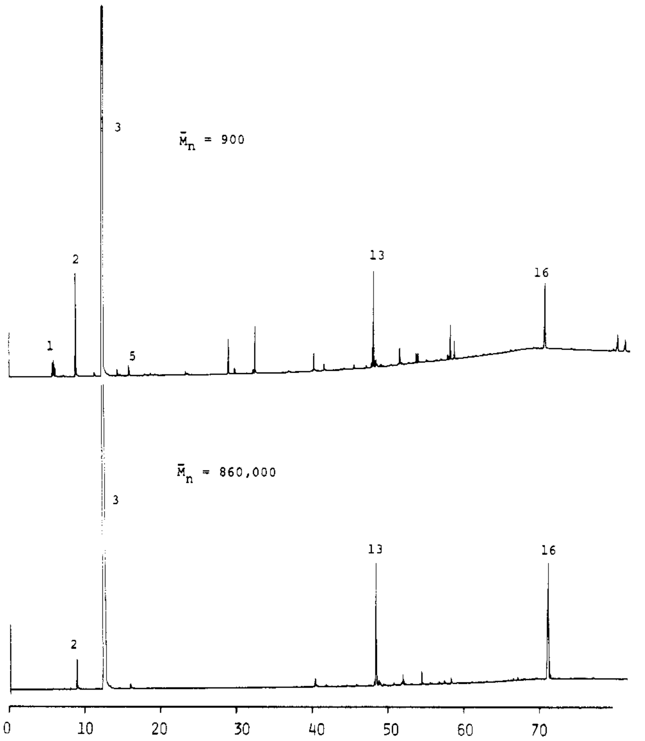

Figure 4. High-resolution pyrograms of linear PS's. Peak numbers are consistent with those in Table II.

calculated as the peak intensity ratio of *m-,p*-EST against *m-,p*-DVB on the pyrogram of sample H.

In both cases in Figures 2 and 3, the resulting calibration curves show fairly good linearity and could be used for the determination of the associated isomer contents in the copolymers with various degree of networks.

Characterization of Network Structures of the Copolymers. As discussed in the previous section, the DVB contents in the copolymers, which are closely related to the density of the networks, are easily determined by use of the associated degradation products on the pyrograms. On the other hand, the linear portions of the networks between the cross-linking points of the copolymers consist of ST and EST sequences. It is known that PS, which has long ST sequences, yields ST monomer, dimer, and trimer on the pyrogram and that their yields change as a function of the average molecular weight (MW).[11,12] In the following, eight kinds of monodisperse PS's ranging from $\bar{M}_n$ ($\approx\bar{M}_w$) = 900 to 860 000 were utilized as reference polymers for estimating the $\bar{M}_w$ of ST sequences in the networks of the copolymers.

Figure 4 shows typical pyrograms of PS's with two extreme $\bar{M}_n$ (900 and 860 000). In addition to the main degradation products such as ST monomer, dimer, and trimer, various satellite peaks are observed. Table III summarizes the observed yields (Y) of monomer, dimer, and trimer together with those of toluene. Y is defined as the associated peak intensity (counts) normalized by the ST content (μg) in the sample used for the measurement. As can be seen from the recovery data in Table III, the PS samples with $\bar{M}_n$ of more than 10 000 are almost quantitatively recovered on the pyrograms as the peaks of the degradation products, while the recovery decreases for the PS's with lower $\bar{M}_n$. The latter phenomenon should mostly be attributed to the competitive processes between thermal degradation and thermal volatilization of the sample molecules. The contribution of thermal volatilization of the sample becomes significant for the PS's with lower $\bar{M}_n$. The observed data for PS's with $\bar{M}_n$ = 900 and 2 030 suggest that about 23% and 16% of the original samples could not be eluted from the separation column, respectively. Considering this phenomenon, the yields corrected by the recovery rates are given in parentheses in Table III. In the following discussion, these corrected yields are used instead of the observed yields.

Table III
Yield of Pyrolyzates for Linear PS's

MW of PS samples	obsd yield[a]				recovery,[b] %
	Y_{tol}	$Y_{monomer}$	Y_{dimer}	Y_{trimer}	
900	149	3 000	200	184	76.5
	(194)	(3 920)	(261)	(241)	
2 030	141	3 450	255	248	83.6
	(169)	(4 130)	(305)	(297)	
10 300	76	4 370	366	415	99.3
	(77)	(4 400)	(368)	(418)	
51 000	54	4 420	372	482	99.7
	(54)	(4 440)	(373)	(484)	
97 200	51	4 380	369	494	99.1
	(52)	(4 420)	(372)	(499)	
860 000	49	4 440	359	481	99.4
	(50)	(4 460)	(361)	(484)	

[a] Y is defined as the associated peak intensity (count) normalized by the ST content (μg) in the sample used for the measurement. The data in parentheses are corrected values for the recovery. [b] The recovery (%) is defined as the total peak intensity on the pyrogram normalized by the sample amount (μg) when the value for poly(α-methylstyrene) is regarded as 100%.

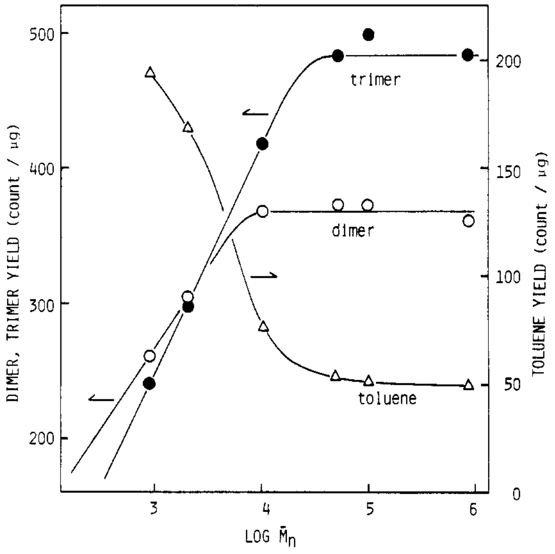

Figure 5. Relationship between dimer, trimer, and toluene yields and $\bar{M}_n$ of linear PS's.

Generally, the corrected yields of the characteristic products listed in Table III change as monotonous functions of $\bar{M}_n$ of PS's. Among these, Figure 5 illustrates the relationships between $\bar{M}_n$ and the corrected yields for toluene, dimer, and trimer, whose changes are significantly large. The yield of toluene (Y_{tol}) decreases monotonously with the increase in $\bar{M}_n$ since the formation of toluene is closely related with the molecular terminals of PS's. On the other hand, the yields of dimer and trimer increase with the rise of $\bar{M}_n$ since they are primarily formed through radical transfer of the macroradicals with long ST sequences. As can be seen in Figure 5, the relation associated with the yield of trimer shows a wider dynamic range than that of dimer.

Table IV summarizes the observed yields of the characteristic products from the ST–DVB copolymers corresponding to Table III. Although the monomer yields are almost constant regardless of the degree of cross-linking,

Table IV
Yield of Pyrolyzates for ST-DVB Copolymers

		obsd yield			
sample	DVB, wt %	Y_{tol}	Y_{monomer}	Y_{dimer}	Y_{trimer}
A	1.0	53	4280	376	444
B	2.0	57	4290	356	425
C	10.0	81	4520	283	302
D	18.0	97	4570	214	195
E	25.0	103	4340	154	123
F	33.0	128	4250	101	72
H	11.0	64	4140	255	329

those for toluene, dimer, and trimer show significant changes depending on the expected networks of the copolymers.

Before developing comparative discussion between the yields of the common characteristic products from linear PS's and the ST-DVB copolymers, we will consider the thermal behaviors of the copolymers observed by TGA. Figure 6 shows TG curves for the copolymer samples A, C, E, F, and G. The initial weight loss around 400 °C shifts to higher temperature with increasing DVB content. The amount of residues also changes as a function of DVB content. These facts suggest that the thermal stability of the copolymers increases as DVB content increases. However, it could be considered that the ST sequences in the networks behave similarly to those of the corresponding linear PS's during the thermal degradation at such a high temperature as 590 °C since the C–C bonds near the cross-linking points are the most susceptible to thermal cleavages that give linear macroradicals with the corresponding ST sequences contained between the network structures. From this point of view, provided that the distribution of the ST sequences between the networks is narrow enough, the $\bar{M}_w$ of the ST sequences between the networks could be estimated by comparing the yields of the common characteristic products from the monodisperse linear PS's with known $\bar{M}_n$ ($\approx\bar{M}_w$). Here, considering the molecular weight distribution of the ST sequences in the sample molecules, the observed yield, Y (counts/μg), of the characteristic products such as dimer, trimer, and toluene from a given sample can be expressed as follows:

$$Y\ (\mathrm{counts}/\mu\mathrm{g}) = \sum y_i w_i / \sum w_i \qquad (3)$$

where y_i (counts/μg) is the formation probability of the characteristic products (dimer, trimer, or toluene) from a ST sequence with molecular weight of M_i of fractional weight w_i (μg) among the whole sample utilized ($\sum w_i$). Since the relationships between the yields and $\bar{M}_n$ shown in Figure 5 are all monotonous functions, the formation probability of the characteristic product, y_i defined in eq 3, can be expressed as a linear function of M_i within a given narrow range of MW.

$$y_i = aM_i + b \qquad (4)$$

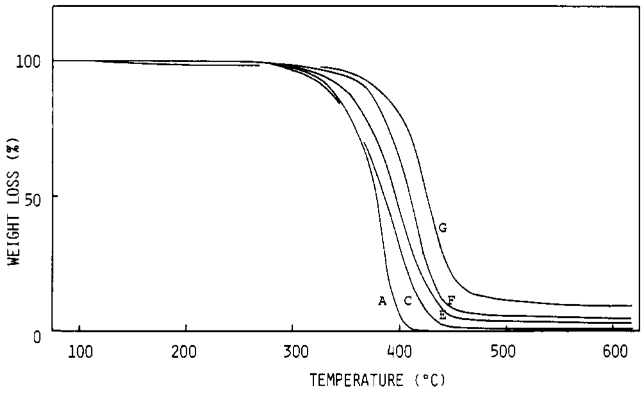

Figure 6. TG curves of ST–DVB copolymers.

where a and b can be regarded as constants within the narrow range of MW. When eq 3 and 4 are joined, the observed yield for the characteristic product can be expressed as follows:

$$Y = \sum(aM_i + b)w_i/\sum w_i = a\sum M_i w_i/\sum w_i + b = a\bar{M}_w + b \qquad (5)$$

This derived equation suggests that the observed yield has a close relation to the weight-average molecular weight ($\bar{M}_w$) of the sample within a limited range of MW.

Table V shows the estimated $\bar{M}_w$ of ST sequences between cross-linking points in the copolymers by applying the data in Table IV to the calibration curves in Figure 5. The $\bar{M}_n$ values between the networks by DSC, the recovery data by PyGC, and the observed residues on TGA are also listed in Table V. The rough $\bar{M}_n$ values were calculated by using the following equation reported by Nielsen:[13]

$$T_g - T_{g0} = 3.9 \times 10^4/\bar{M}_n \qquad (6)$$

where T_g and T_{g0} are the glass transition temperatures of the copolymers and a linear PS with infinite molecular weight, respectively. Although, as shown in Figure 7, the relationship between observed T_g's by DSC and DVB contents changes almost linearly, the equation was only applied for the copolymers with lower DVB contents. As shown in Table V, the residues on TGA are much smaller than the amount of unrecovered sample on the pyrograms. These discrepancies should be attributed mainly to the fractions that degraded into relatively larger fragments and did not elute from the separation column in PyGC.

Among the $\bar{M}_w$ values observed by PyGC, those obtained from dimer and trimer are comparable with each other, while those from toluene are generally much greater than the others since the toluene yields from the ST sequences in the network structures are much more suppressed than those from linear molecules with free terminals. On the whole, both the estimated $\bar{M}_w$ and $\bar{M}_n$ values between the

Table V
Estimated Styrene Sequences between Cross-Linking Points in ST-DVB Copolymers

		$\bar{M}_w$ of ST sequences between networks[a]					
sample	DVB, wt %	from dimer yield	from trimer yield	from toluene yield	$\bar{M}_n$ between networks from T_g by DSC	recovery on pyrogram,[b] %	residue on TGA, wt %
A	1.0	>10 000 (>100)	15 000 (140)	62 000 (620)	20 000	96.4	
B	2.0	5 200 (50)	11 000 (110)	27 000 (260)	7 500	95.7	
C	10.0	1 300 (13)	2 100 (20)	9 300 (89)	1 900	93.8	0.7
D	18.0	370 (3.6)	490 (4.7)	6 800 (65)		87.5	2.2
E	25.0	120 (1.2)	180 (1.7)	6 200 (60)		78.4	3.1
F	33.0	<100 (<1.0)	<100 (<1.0)	4 400 (42)		71.4	4.7
H	11.0	800 (7.7)	3 100 (30)	13 000 (130)	1 700	90.4	0.9

[a] The data in parentheses are ST units. [b] The recovery (%) is defined as that in Table III.

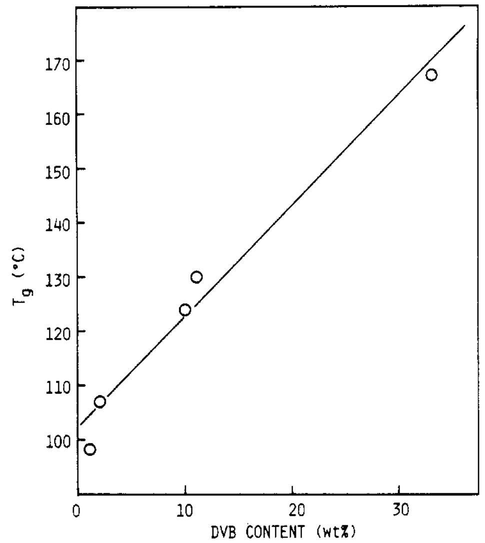

Figure 7. Relationship between T_g and DVB content of ST-DVB copolymers.

networks exhibit basically the same tendency as monotonous functions of the DVB content in the copolymers. Here, considering the polydispersity of the ST sequences between the networks, $\bar{M}_w/\bar{M}_n$ should be much greater than unity. However, the estimated $\bar{M}_w$'s from dimer and trimer yields are lower than those expected from the $\bar{M}_n$ obtained from T_g values. These discrepancies might be attributed to the following reasons: (a) The roughly estimated $\bar{M}_n$'s from T_g values contain the contribution of EST sequences to some extent depending on the composition of the copolymers. (b) The ST sequences in the networks may behave differently rather than similarly to those in linear PS's during their thermal degradation even at high temperatures around 600 °C. (c) The molecular weight distribution of the ST sequences between the networks is too wide to adopt eq 5 where the distribution range is regarded to be narrow enough.

In order to confirm these possible reasons, various ST-DVB copolymers synthesized anionically and their precursor PS's are currently under investigation by PyGC.

Acknowledgment. We are indebted to Showa-Denko Industry Inc. and Toyo-Soda Industry Inc. for providing the various ST-DVB copolymers. We also thank K. Matsumoto for GC-MS measurements and helpful discussion. Financial support in the form of a Grant-in-Aid from the Ministry of Education is gratefully acknowledged.

References and Notes

(1) Rietsch, F.; Froelich, D. *Polymer* **1975**, *16*, 873.
(2) Rietsch, F.; Daveloose, D.; Froelich, D. *Polymer* **1976**, *17*, 859.
(3) Rietsch, F.; Brault, A.; Froelich, D. *Polymer* **1978**, *19*, 1043.
(4) Brault, A.; Rietsch, F.; Froelich, D. *Polymer* **1978**, *19*, 1047.
(5) Rietsch, F. *Macromolecules* **1978**, *11*, 477.
(6) Rietsch, F.; Froelich, D. *Eur. Polym. J.* **1979**, *15*, 349.
(7) Rietsch, F.; Froelich, D. *Eur. Polym. J.* **1979**, *15*, 361.
(8) Sellier, N.; Jones, C. E. R.; Guiochon, G. In "Analytical Pyrolysis"; Jones, C. E. R., Cramers, C. A., Eds.; Elsevier: Amsterdam, 1977.
(9) Popov, G.; Haüsler, K. G.; Krauss, D.; Schuwachula, G. *Plaste Kautsch.* **1980**, *27*, 614.
(10) Sugimura, Y.; Tsuge, S. *Anal. Chem.* **1978**, *50*, 1968.
(11) Tsuge, S.; Okumoto, T.; Takeuchi, T. *J. Chromatogr. Sci.* **1969**, *7*, 250.
(12) Ohtani, H.; Tsuge, S.; Matsushita, Y.; Nagasawa, M. *Polym. J. (Tokyo)* **1982**, *14*, 495.
(13) Nielsen, L. E. *J. Macromol. Sci., Rev. Macromol. Chem.* **1969**, *3*, 69.

Heterogeneity in Branching: Mathematical Treatment of the Amylopectin Structure

Walther Burchard* and Angelika Thurn

Institute of Macromolecular Chemistry, University of Freiburg, Freiburg, FRG.
Received October 22, 1984

ABSTRACT: Heterogeneity in the branching density of amylopectin was disclosed 15 years ago by enzymatic debranching experiments. The question whether such heterogeneity has significant influence on the angular dependence of scattered light from the non-degraded molecule is examined in the present paper. On the basis of cascade branching theory, the two molecular weight averages M_w and M_n, the mean-square radius of gyration $\langle S^2\rangle_z$, and the particle scattering factor $P_z(q)$ have been calculated for the following three models discussed in the literature: (i) the homogeneous Meyer Model, (ii) the heterogeneously branched French model, and (iii) a modified heterogeneously branched structure suggested by Robin and Mercier. The model calculations were carried out under the constraint of the same average branching density as found experimentally. This constraint, together with the experimentally observed length of branches of 22, 44, and 66 units, leads to the existence of densely branched clusters with three to four branching points on the average. Excellent agreement is obtained with the modified Robin-Mercier model, where the chains connecting the cluster carry on the average 1.4 clusters.

Introduction

Polymer science is now a highly developed field, but there still exist a few products, mainly of natural origin, for which, in spite of immense effort, the structure is not sufficiently well-known. The energy-storing biopolymers amylopectin (AP) and glycogen are typical examples. Both of these polysaccharides are highly branched, and the complexity in structure compared to linear chains is considerable.

At first sight, it might appear hopeless ever to find a satisfactory theory of the properties of branched polymers. This is, however, not true for synthetic polymers, where branching occurs essentially at random. This randomness facilitates the application of statistical methods,[1-5] and many properties of synthetic branched resins can now be described very satisfactorily[6] by the Flory-Stockmayer theory. More difficult is the treatment of a branched structure that is subject to incisive constraints[7,8] or that

0024-9297/85/2218-2072$01.50/0